Molecular Genetics and Metabolism Reports 24 (2020) 100604

Contents lists available at ScienceDirect

Molecular Genetics and Metabolism Reports

journal homepage: www.elsevier.com/locate/ymgmr

Intravenous delivery for treatment of mucopolysaccharidosis type I: A comparison of AAV serotypes 9 and rh10

Lalitha R. Belur[a,*], Kelly M. Podetz-Pedersen[a], Thuy An Tran[a], Joshua A. Mesick[a], Nathaniel M. Singh[a], Maureen Riedl[b], Lucy Vulchanova[b], Karen F. Kozarsky[c,1], R. Scott McIvor[a]

[a] Center for Genome Engineering, Department of Genetics, Cell Biology and Development, University of Minnesota, 6-160 Jackson Hall, Church St. S. E, Minneapolis, MN 55455, USA
[b] Department of Neuroscience, University of Minnesota, 6-145 Jackson Hall, Church St. S.E, Minneapolis, MN 55455, USA
[c] REGENXBIO Inc., 9600 Blackwell Road, Suite 210, Rockville, MD 20850, USA

ARTICLE INFO

Keywords:
Gene therapy
AAV9
AAVrh10
Mucopolysaccharidosis Type I (MPS I)
Iduronidase (IDUA)
Intravenous delivery

ABSTRACT

Mucopolysaccharidosis type I (MPS I) is an inherited metabolic disorder caused by deficiency of alpha-L-iduronidase (IDUA), resulting in accumulation of heparan and dermatan sulfate glycosaminoglycans (GAGs). Individuals with the most severe form of the disease (Hurler syndrome) suffer from neurodegeneration, intellectual disability, and death by age 10. Current treatments for this disease include allogeneic hematopoietic stem cell transplantation (HSCT) and enzyme replacement therapy (ERT). However, these treatments do not address CNS manifestations of the disease. In this study we compared the ability of intravenously administered AAV serotypes 9 and rh10 (AAV9 and AAVrh10) for delivery and expression of the IDUA gene in the CNS. Adult C57BL/6 MPS I mice were infused intravenously with either AAV9 or AAVrh10 vector encoding the human IDUA gene. Treated animals demonstrated supraphysiological levels and widespread restoration of IDUA enzyme activity in the plasma and all organs including the CNS. High levels of IDUA enzyme activity were observed in the plasma, brain and spinal cord ranging from 10 to 100-fold higher than heterozygote controls, while levels in peripheral organs were also high, ranging from 1000 to 10,000-fold higher than control animals. In general, levels of IDUA expression were slightly higher in peripheral organs for AAVrh10 administered animals although these differences were not significant except for the lung. Levels of IDUA expression between AAV 9 and rh10 were roughly equivalent in the brain. Urinary and tissue GAGs were significantly reduced starting at 3 weeks after vector infusion, with restoration of normal GAG levels by the end of the study in animals treated with either AAV9 or rh10. These results demonstrate that non-invasive intravenous AAV9 or AAVrh10-mediated IDUA gene therapy is a potentially effective treatment for both systemic and CNS manifestations of MPS I, with implications for the treatment of other metabolic and neurological diseases as well.

1. Introduction

The mucopolysaccharidoses are a group of rare inherited lysosomal disorders caused by lysosomal enzyme deficiency leading to aberrant glycosaminoglycan (GAG) catabolism [1,2]. This results in abnormal GAG accumulation in the lysosomes leading to progressive cellular damage in multiple organ systems. Mucopolysaccharidosis type I is caused by deficiency of α-L-iduronidase (IDUA), with a disease spectrum that ranges from mild to severe [3]. The most severe form of the disease, Hurler syndrome (MPS IH), is also the most prevalent, with an incidence of 1:100,000. Accumulation of heparan and dermatan sulfate GAG leads to systemic disease, multiple organ failure, severe neurocognitive impairment, and death by age 10. MPS IH is effectively treated by allogeneic hematopoietic stem cell transplantation (HSCT), with engrafted donor cells providing a source of enzyme for metabolic cross-correction [4–11]. HSCT thus constitutes a remedy for many of the manifestations of MPS IH, and when carried out early in life reduces the rate of cognitive decline. Intermediate (Hurler-Scheie) and mild (Scheie) forms of MPS I are treated by enzyme replacement (ERT) [12–16], providing systemic relief from metabolic storage disease. Nonetheless, skeletal and cardiac abnormalities as well as neurologic and other problems persist for MPS I individuals, prompting the search for more effective therapies.

A natural extension of allogeneic HSCT for MPS I is instead

* Corresponding author.
E-mail address: belur001@umn.edu (L.R. Belur).
[1] Current affiliation: SwanBio Therapeutics Inc.

https://doi.org/10.1016/j.ymgmr.2020.100604
Received 4 May 2020; Accepted 5 May 2020

transplantation with autologous HSC that have been genetically restored *ex vivo* for IDUA expression [17–20]. Direct *in vivo* IDUA gene transfer has also been reported using lentiviral, retroviral and adeno-associated (AAV) virus vectors in adult and neonatal MPS I mice, in dogs and non-human primates [21–36]. Achieving effective delivery of enzyme to the central nervous system has been an important goal in the development of genetic therapies for MPS I. Studies in the murine model of MPS I have demonstrated the effectiveness of intracerebroventricular and intrathecal introduction of IDUA-transducing AAV vector [23,26,28,29,35], and even intranasal administration resulted in wild-type levels of IDUA in the brain [33]. CNS-directed gene transfer has recently shown promise in large animal studies in which IDUA-transducing AAV9 was delivered intracisternally in non-human primates [35,36].

Intravenously administered AAV is broadly distributed, and evidence that AAV vectors packaged using capsid serotypes 9 and rh10 can cross the blood-brain barrier [37–42] additionally raises the prospect for the potential effectiveness of intravenous delivery as a non-invasive means of achieving transduction of CNS tissues to address neurologic manifestations of human disease. Most notable are the results of a clinical trial for the most severe form of spinal muscular atrophy, in which patients received a single intravenous administration of scAAV9 containing spinal motor neuron 1 cDNA, resulting in significant impact on lifespan, motor function and overall disease [43].

In this paper, we compared the relative therapeutic effectiveness of IDUA-transducing AAV9 and AAVrh10 on IDUA enzyme expression systemically and in the brain after intravenous administration. With a single intravenous injection of AAV vector, we achieved extremely high levels of IDUA enzyme in the circulation, with concomitant high and widespread levels of IDUA enzyme activity in all tissues tested with both serotypes, including the CNS. We observed metabolic correction and clearance of lysosomal storage materials with both serotypes. These results have strong implications for effective, non-invasive genetic therapy of MPS I, especially with respect to neurological manifestations of the disease.

2. Materials and methods

2.1. Vector constructs and packaging

Generation of the miniCAGS regulated IDUA (AAV-MCI) expression cassette (pTR-MCI) has been described previously [26]. This vector was packaged into AAV9 and AAVrh10 virions at the University of Pennsylvania vector core, generating recombinant (r) AAV9-IDUA and AAVrh10-IDUA. Vector titer was 1.1×10^{13} genome copies/ml for AAV9-IDUA and 1.7×10^{13} genome copies/ml for AAVrh10-IDUA.

2.2. Animals and intravenous infusions

The MPS I mouse strain was generously provided by Dr. E. Neufeld [51]. IDUA−/− offspring were generated from homozygous IDUA−/− breeding pairs. Animals were maintained under specific pathogen-free conditions in AAALAC-accredited facilities. All animal work was reviewed and approved by the Institutional Animal Care and Use Committee of the University of Minnesota. MPS I IDUA-deficient animals ranging in age from 8 weeks to 21 weeks were infused through the tail vein with 1×10^{12} vector genomes of AAV9-IDUA (5 animals, 4 males and 1 female) or AAVrh10-IDUA (5 animals, 4 males and 1 female). In order to avoid anti-IDUA and anti-capsid immune responses, all animals (including untreated controls) were immunosuppressed by weekly intraperitoneal injection of 120 mg/kg cyclophosphamide (CP), starting 3 days after vector infusion. Mice were weighed regularly and if more than 10% of their body weight was lost, CP injections were withdrawn until body weight was regained. Blood was collected every 1–2 weeks by venipuncture and processed to plasma. Urine was also collected at 1–2 week intervals. Both plasma and urine were stored at -20 °C until assayed for IDUA and GAGs, respectively.

Animals were sacrificed at 10 weeks post-injection, transcardiacally perfused with 50 ml PBS, and tissues (heart, liver, kidney, lung, spleen and microdissected brain) collected. Tissues were frozen on dry ice and stored at -20 °C until processed. Tissue lysates were prepared as described previously [33]. Briefly, tissues were homogenized in 0.9% saline using a bullet bead blender, and homogenates were clarified by centrifugation in an Eppendorf centrifuge at 13,000 rpm for 15 min. Supernatants (tissue lysates) were transferred to clean tubes and stored at -20 °C until assayed for IDUA and GAGs.

2.3. IDUA enzyme assay

Plasma and tissue lysates were assayed for IDUA activity in a fluorometric assay using 4-MU iduronide as substrate (Glycosynth, England), as previously described [26]. Emitted fluorescence was measured in a BioTek Synergy Mx plate reader. Protein was measured using the Pierce assay. Enzyme activity is expressed as nmol 4-methylumbelliferone released per mg protein per hour (nmol/h/mg) and as nmol/h/ml for plasma. Two-way ANOVA with Sidaks's multiple comparison tests were used for all statistical analyses.

2.4. GAG assay

Tissue lysates and urine GAGs were assayed using the Blyscan Sulfated Glycosaminoglycan Assay kit (Accurate Chemical, NY) as described previously [26]. Tissue GAGs were normalized to protein and expressed as μg GAG/mg protein and urine GAGs are expressed as μg GAG/mg creatinine. Creatinine was assayed using the Creatinine assay kit from Sigma.

2.5. Immunohistochemistry

Male mice were deeply anaesthetized and perfused *via* the heart with calcium-free Tyrode's solution (in mM: NaCl 116, KCl 5.4, $MgCl_2{\cdot}6H_20$ 1.6, $MgSO_4{\cdot}7H_2O$ 0.4, NaH_2PO_4 1.4, glucose 5.6, and $NaHCO_3$ 26) followed by fixative (4% paraformaldehyde and 0.2% picric acid in 0.1 M phosphate buffer, pH 6.9). Tissues were dissected from the animal and stored in PBS containing 10% sucrose and 0.05% sodium azide at 4 °C for a minimum of 24 h before being frozen and sectioned at 14 μm thickness using a cryostat. Sections were mounted onto gel-coated slides and stored at -20 °C until further use. For immunohistochemical staining, sections were incubated in diluent (PBS containing 0.3% Triton-X100; 1% bovine serum albumen, 1% normal donkey serum) for 1 h at room temperature followed by incubation in primary antisera overnight at 4 °C. Primary antisera included sheep anti-IDUA (R & D Systems, Minneapolis, MN, 1:500), chicken anti-GFAP (Abcam, Cambridge, MA 1:1000), rat anti-CD31 (BD Pharmingen, San Jose, CA, 1:100) and rabbit anti-NeuN (Abcam, Cambridge, MA, 1:1000). Sections were rinsed in PBS, incubated in species appropriate secondary antisera (Cy2 1:100, Cy3 1:300, Jackson ImmunoResearch, West Grove, CA) for 1 h at room temperature, rinsed again using PBS, and coverslipped using glycerol and PBS containing *p*-phenylenediamine (Sigma). Images were collected using an Olympus Fluoview 1000 confocal microscope and adjusted for brightness and color using Adobe Photoshop software. Upon examination of the labeling, we noted autofluorescence, likely lipofuchsin granules, that was visible at 405 nm, 488 nm, and 565 nm wavelengths of excitation. To distinguish the autofluorescence from immunolabeling that was visualized with 488 nm and 565 nm excitation wavelengths, we also collected images at 405 nm. Merging of the images collected at the three wavelengths resulted in a pseudocolored image where autofluorescence appeared in white.

2.6. Quantitative polymerase chain reaction

QPCR was carried out as described previously [26]. Briefly, genomic DNA was extracted from tissue homogenates using the GeneJET Genomic DNA Purification kit (ThermoFisher Scientific). Reaction mixtures contained 200 ng of DNA, 2× IQ SYBR Green Supermix (Bio-Rad), and 200 nM each of forward and reverse primer. IDUA primers used were forward primer: 5'-AGGAGATACATCGGTACG-3′ and reverse primer: 5'-TGTCAAAGTCGTGGTGGT-3′. PCR conditions were: 95 °C for 2 min, followed by 40 cycles of 95 °C for 40 s, 58 °C for 30 s, and 72 °C for 1 min. The standard curve for IDUA consisted of serial dilutions of plasmid pTR-MCI.

3. Results

3.1. High levels of IDUA enzyme activity in the circulation and in tissues after intravenous injection of AAV9 orAAVrh10

The comparative effectiveness of AAV9- and AAVrh10-mediated IDUA gene delivery after intravenous injection was evaluated in IDUA deficient mice. Animals were immunosuppressed with weekly intraperitoneal administration of 120 mg/kg cyclophosphamide (CP) for 4 weeks starting 3 days after a single intravenous injection of either AAV9-IDUA or AAVrh10-IDUA vector at 2–5 months of age. Blood was collected at 1- to 2-week intervals and plasma assayed for IDUA enzyme activity (Fig. 1A). Enzyme activity was soon (4 days) detected at > 100 nmol/h/ml in plasma of all animals and continued to increase until 70 days post-infusion, when the experiment was terminated. Levels of IDUA activity were similar in both groups of animals. In comparison to wild-type C57BL/6 animals, the mean levels of enzyme activity in AAV-IDUA administered animals ranged from 20-fold higher at 4 days post-injection to 1000-fold higher by week 4. Levels of enzyme from both serotype administered animals appeared to reach steady state by 4 weeks post-injection, with no significant increase at 8 weeks.

All experimental animals were euthanized 70 days following vector administration and tissues extracted for analysis of vector biodistribution, IDUA expression and its effect on lysosomal storage materials. The brain was microdissected at harvest to determine comparative distribution and enzyme expression in different regions of the CNS. IDUA enzyme activity was undetectable both in the brain and peripheral organs of IDUA deficient animals. Both AAV9 and AAVrh10 serotypes achieved high levels of enzyme in all areas of the brain (Fig. 1B), with IDUA activity ranging from 10 to 100-fold higher than that of normal heterozygote control animals. IDUA activity was generally equivalent in all areas of the brain, although levels of expression were lowest in the olfactory bulb for both AAV9 and rh10. No significant differences were observed between serotypes.

Enzyme levels in peripheral organs of treated animals ranged from 100 to 10,000-fold higher than normal heterozygote levels. IDUA activities in general, trended higher for AAVrh10 than AAV9 in all organs tested (Fig. 1C). However, differences in enzyme levels between serotypes were not significant.

3.2. Vector biodistribution

Vector biodistribution was determined by qPCR of tissue DNA extracts for the human IDUA cDNA sequence. In general, the level of observed transduction corresponded with the level of tissue IDUA

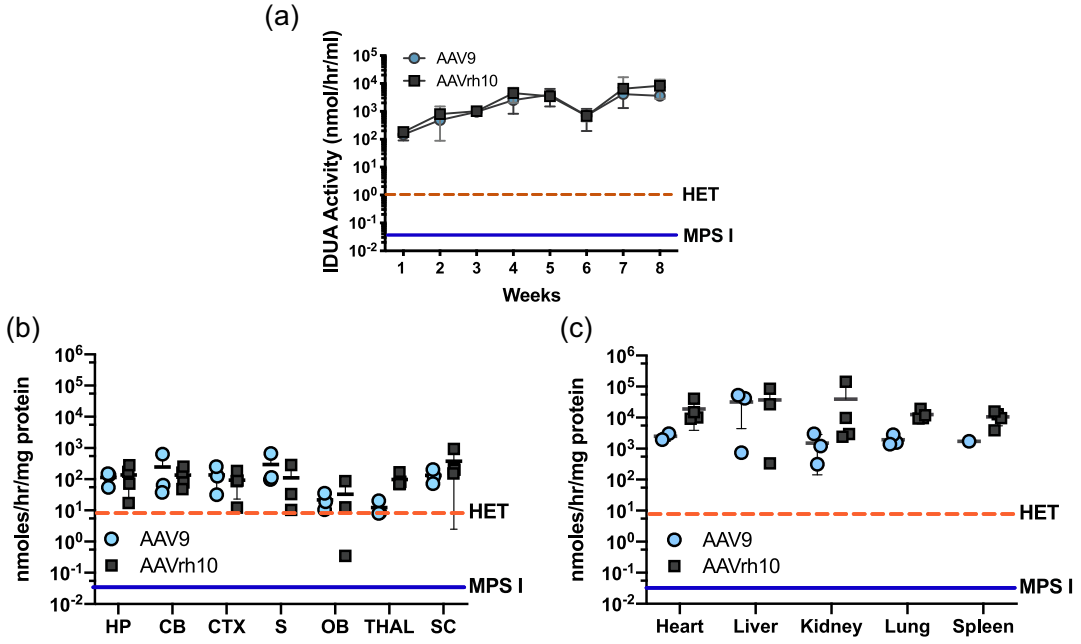

Fig. 1. IDUA Activity in plasma and tissues after intravenous administration of AAV9 and AAVrh10 vectors delivering the IDUA gene. (A) Enzyme activity in plasma. Blood was collected at 1 to 2 week intervals and plasma was assayed for IDUA activity. High and sustained levels of IDUA activity were seen in plasma from animals treated with bith serotypes (n = 5; each serotype). The level of plasma IDUA activity in normal heterozygotes (n = 4) is indicated by a dashed line and ranges from 0.5–2 nmoles/hr/ml. Enzyme activity in plasma from MPS I animals (n= 4) was undetectable (< 0.05 nmoles/hr/ml). Bars represent means +/− SD. (B) IDUA enzyme activity in brain No CR.

Brains were micro-dissected and extracts assayed for IDUA enzyme activity. There was widespread IDUA activity in the brains of treated animals (n = 5) compared to wild type animals. Enzyme activity found in normal heterozygotes (n = 4) is indicated by the dashed line, and ranges from 1 to 15 nmoles/h/mg in the brain. Enzyme activity was not detected in untreated MPS I animals (< 0.05 nmoles/h/mg, n = 4). Mean +/− SD values are represented by bold horizontal lines and light vertical lines respectively. HP, hippocampus; CB, cerebellum; CTX, cortex; S, striatum; OB, olfactory bulb; THAL, thalamus; SC, spinal cord. No CR.

(C) IDUA enzyme activity in peripheral organs. Levels of IDUA activity were extremely high in peripheral organs of mice from treated animals. The range of enzyme activities found in normal heterozygotes is indicated by the dashed line, and ranges from 1-15 nmoles/hr/mg. Enzyme activity was not detected in untreated animals (< 0.05 nmoles/hr/mg).

Mean +/− SD values are represented by bold horizontal lines and light vertical lines respectively.

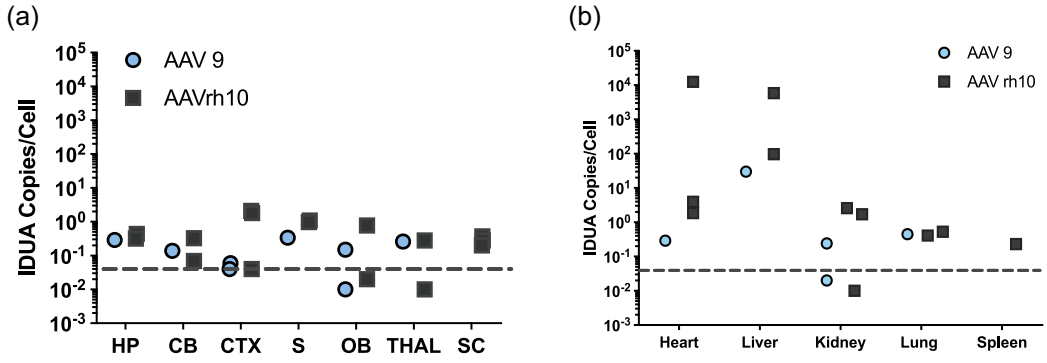

Fig. 2. Vector biodistribution. Tissue DNA extracts were assayed for the presence of IDUA sequences by quantitative PCR. Each symbol represents 1 animal. Dashed line indicates the lower limit of detection analyzed from genomic DNA samples collected from heterozygote controls (< 0.05). (A) IDUA vector sequences in brain and spinal cord. HP, hippocampus; CB, cerebellum; CTX, cortex; S, striatum; OB, olfactory bulb; THAL, thalamus; SC, spinal cord. (B) IDUA vector sequences in peripheral organs.

activity summarized above. The highest vector level was observed in the liver (50–1000 vc/diploid genome) and in the heart (0.5-1000 vc/diploid genome; Fig. 2A), with somewhat reduced levels detected in other peripheral tissues. Vector sequences in micro-dissected portions of the brain ranged from 0.05–1 vc/diploid genome (Fig. 2B).

3.3. Immunohistologic analysis of IDUA expression

Experimental animals were perfusion-fixed, and then peripheral and CNS tissues were evaluated for IDUA expression using anti-IDUA antibody as previously described [26]. High levels of IDUA immunoreactivity (−ir) were observed in the liver of both AAV9 and AAVrh10-treated animals (Fig. 3A-C). In the brain, we observed sparse IDUA-labeled structures with a fairly uniform distribution in different regions. The pattern of labeling was similar in AAV9 and AAVrh10-treated mice. In double-labeling experiments, we did not observe evidence for colocalization of IDUA-ir and labeling for markers of neurons (NeuN, Fig. 3, D-F), astrocytes (GFAP, Fig. 3G-I), or microglia (Iba1, not shown).

However, the relationship of IDUA-ir relative to GFAP-ir suggested that IDUA-ir is localized in close proximity to astrocyte endfeet associated with blood vessels. This observation was confirmed by double-labeling for IDUA and the endothelial marker CD31, although IDUA- and CD31-ir did not colocalize (Fig. 3, J-L).

Taken together, these observations suggest that in the CNS parenchyma IDUA-ir is most likely localized in pericytes, which represent the third cellular component of the neurovascular unit. IDUA-ir was also observed in the choroid plexus of both AAV9- and AAV10-treated mice (not shown). The labeling appeared to be associated with the vasculature rather than the epithelial cells of the choroid plexus.

3.4. Effect of iduronidase expression on glycosaminoglycan accumulation

The high level IDUA activity observed in the brain and peripheral organs was associated with a decrease in GAG excretion and storage throughout the body. Urine was collected weekly from all animals starting at time of treatment until termination of the experiment at 70 days post-treatment.

Normalization of urine GAG excretion was seen by Day 14 in both treatment groups ($P < .05$ for both groups) (Fig. 4A). GAG levels in urine were similar in both treatment groups, although slightly but not significantly lower for AAV9-IDUA treated animals.

GAG levels were significantly reduced in all parts of the brain in both treatment groups compared to untreated animals ($P < .05$ to 0.0001 for both groups), although not completely.

normalized (Fig. 4B).

In peripheral organs, GAG levels were completely normalized in both treatment groups (non-significant *vs* Het) (Fig. 4C). There was no significant difference between the two serotypes with respect to normalization of GAG levels.

4. Discussion

Extremely high levels of IDUA were observed in all tissues evaluated, including the brain, after a single intravenous injection of 1×10^{12} vector genomes of either AAV serotype 9 or serotype rh10 transducing the human IDUA sequence. High levels of enzyme were accompanied by normalization of GAG levels in all peripheral tissues, and a significant reduction of GAGs in the brain. While GAG levels in the brain were normalized, or close to normalized in the hindbrain (cerebellum and spinal cord; Fig. 4B), GAG levels were reduced but not normalized in other parts of the brain. However, levels of IDUA enzyme activity were roughly equivalent across the brain (Fig. 1B) as well as in quantitated vector DNA (Fig. 2), indicating a lack of IDUA penetration into certain areas of the brain where GAGs persist. IDUA immunofluorescence demonstrated that transduction was widespread in the liver and heart, and while transduction was observed in brain, the labeling appeared to be largely associated with blood vessels. These observations suggest that IDUA activity in the CNS is most likely the result of enzyme diffusion after overexpression in the CNS vasculature and/or of uptake from the circulation. However, we cannot rule out expression of IDUA in neurons or glia that is below the level of detection by immunofluorescence.

Different routes of AAV delivery can be used to access the CNS. While direct intracranial injection into brain parenchyma circumvents the blood brain barrier, subsequent vector spread is diffusion-dependent, resulting in localized and limited vector distribution. Injection at multiple sites is thus required to achieve greater vector distribution, with each injection requiring a craniotomy [44,45]. Widespread vector delivery can be achieved through the cerebrospinal fluid by intracerebroventricular (ICV), intracisterna magna (ICM), or lumbar injection. While there are conflicting data regarding lumbar injection in larger animals, the ICV and ICM routes, although invasive, lead to widespread AAV mediated transduction in the CNS, especially with AAV serotypes 9 and rh10 [46–50].

Intravenous injection is the least invasive and the most promising alternative route of vector administration, especially since AAV9 and rh10 transduce a wide variety of cell types and are also known to cross the blood brain barrier (BBB). Foust et al. [37] and Duque et al. [38] have demonstrated in both neonatal and adult mice, that AAV9 penetrates the BBB and leads to widespread transduction and gene expression in the CNS. Zhang et al. [42] have also shown that intravenous administration of AAV rh10 leads to extensive distribution and widespread gene expression in the brain. AAV9 has been tested extensively

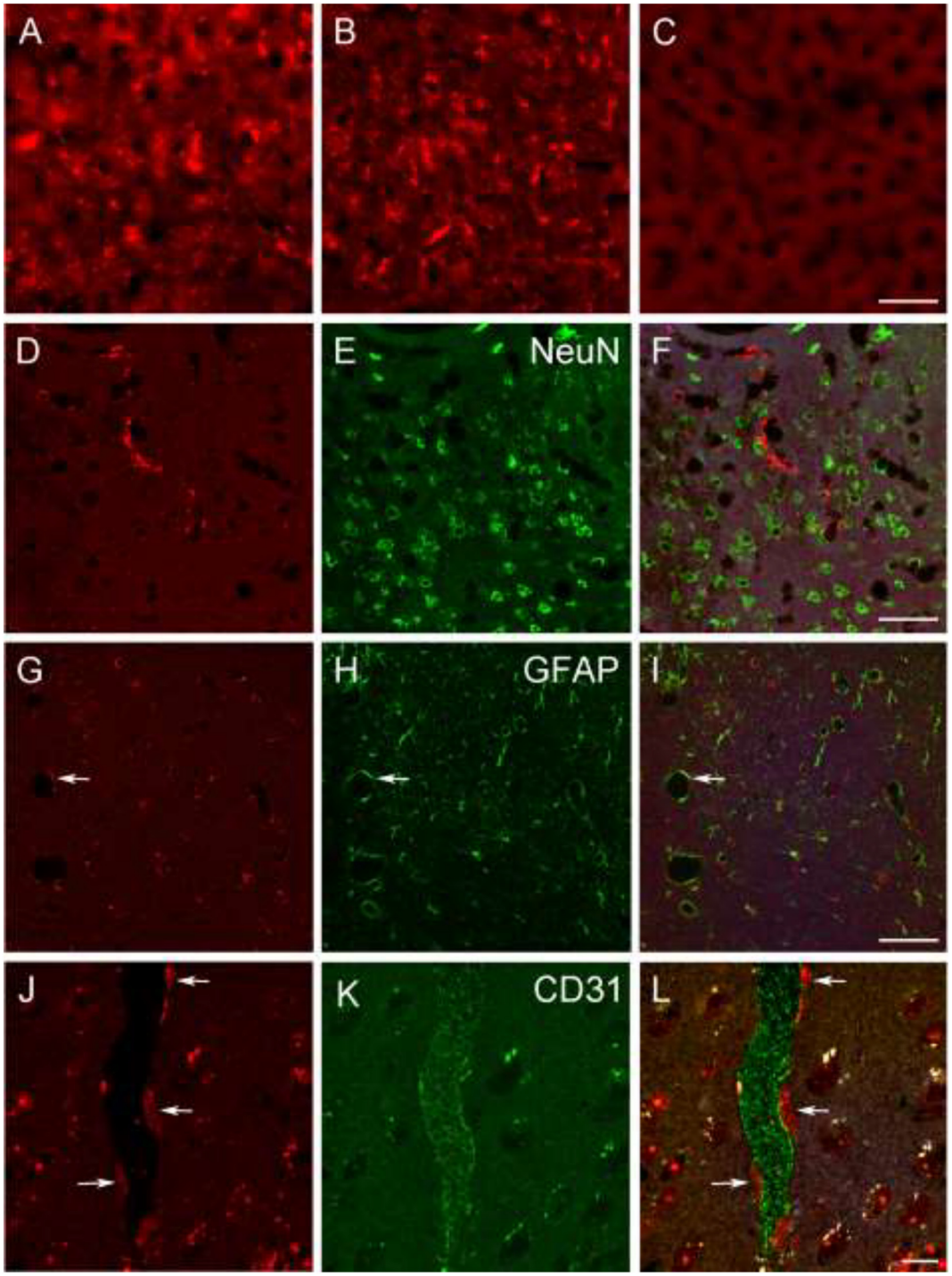

Fig. 3. Immunohistologic analysis of IDUA expression. A-C, IDUA immunoreactivity (−ir) was abundant in livers from AAV9- (A) and AAVrh10 (B)-treated mice, while labeling was absent in liver from an untreated MPS I mouse (C). Scale bar: 50 μm. D-F, A representative image of double-labeling for IDUA (D) and the neuronal marker NeuN (E), showing lack of colocalization (F) in the cortex of an AAV9-treated mouse. Scale bar: 50 μm. G-I, A representative image of double-labeling for IDUA (G) and the astrocyte marker GFAP (H), showing lack of colocalization (I) in hippocampus of an AAVrh10-treated mouse. Arrows indicate an example of a blood vessel with closely associated IDUA- and GFAP-ir. Scale bar: 50 μm. J-L, Double-labeling for IDUA (J) and the endothelial marker CD31 (K) in cortex of an AAV9-treated mouse reveals apparent IDUA-positive cellular profiles that are closely associated with a CD31-ir blood vessel. White puncta correspond to autofluorescent structures. Scale bar: 10 μm.

by intravenous delivery in several animal species including newborn/infant/adult rodents, cats, dogs, and non-human primates [47]. Despite the discrepancy in cell transduction profile between the different species, these results corroborate the therapeutic capability of non-invasive, intravenous AAV9-mediated gene delivery for CNS diseases. Significant therapeutic results have also been shown for intravenous AAV9 treatment of adult mice in models of MPS II [48], MPS IIIA [52] and IIIB [53], MPS VII [54], GM1 gangliosidosis [55], Sandhoff disease [56], multiple sulfatase deficiency [57], and metachromatic leukodystrophy [58].

While the studies cited above report transduction of brain tissue after IV AAV delivery, our results in male mice indicate that IDUA

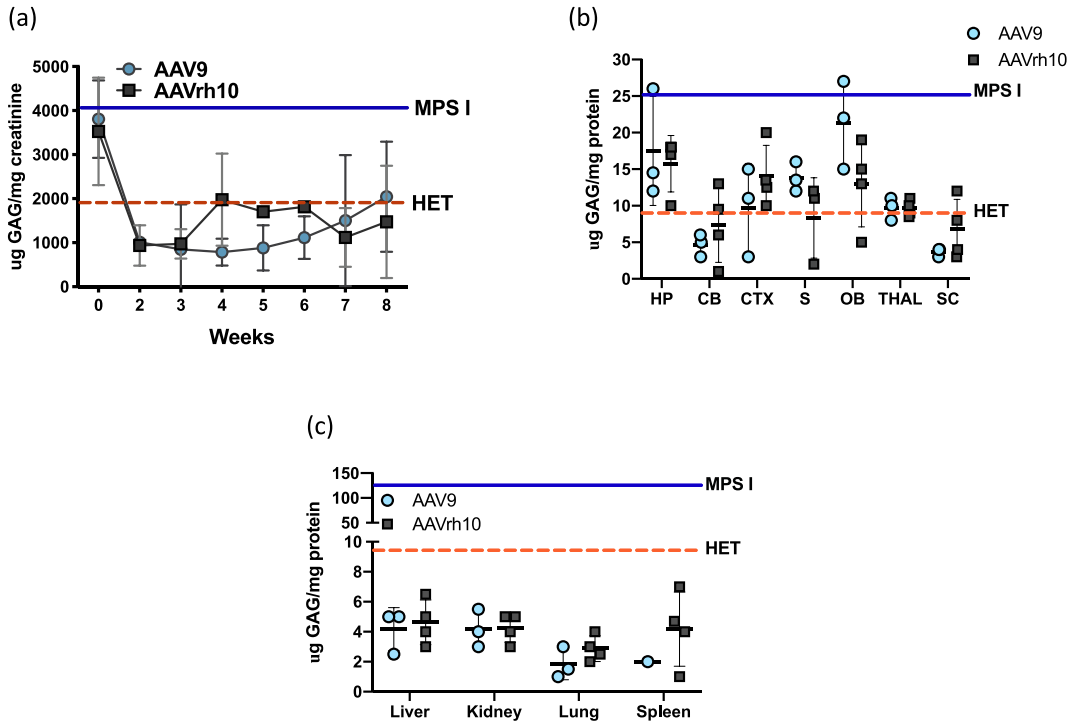

Fig. 4. Glycosaminoglycan storage materials in tissues and in urine post-AAV administration. (A) GAG excretion in urine. Urine was collected at 1 to 2-week intervals and assayed for glycosaminoglycans. The levels of GAGs found in untreated MPS I mice ranged from 4000 to 6000 μGAG/mg creatinine and in normal heterozygotes ranged from 300 to 2000 μGAG/mg creatinine, and are indicated by solid and dashed horizontal lines, respectively. Bars represent means +/− SD. (B). GAG accumulation in brain. Tissue lysates from different parts of the brain were assayed for GAG storage. GAG levels were normalized in the cerebellum and spinal cord and reduced in other parts of the brain from treated animals. The levels of GAG found in untreated MPS I mice ranged from 15-25 μg GAG/mg protein in the brain, and in normal heterozygotes ranged from 1-10 μg GAG/mg protein, and are indicated by solid and dashed horizontal lines, respectively. Mean +/− SD values are represented by bold horizontal lines and light vertical lines respectively. HP, hippocampus; CB, cerebellum; CTX, cortex; S, striatum; OB, olfactory bulb; THAL, thalamus; SC, spinal cord. (C) GAG accumulation in peripheral organs. Lysates from peripheral tissues showed normalization of GAG levels. The levels of GAG found in untreated MPS I mice ranged from 50-150 μg GAG/mg protein and are indicated by the solid horizontal line. Normal heterozygote levels range from 1-10 μg GAG/mg protein, and are indicated by a dashed horizontal line. Mean +/− SD values are indicated.

expression with both serotypes was limited to the CNS vasculature. Similar to what we report in this manuscript, Schuster et al. [70] report low to undetectable levels of transduction in CNS studies after intravenous delivery in comparison with intrathecal delivery. Other variables may have affected the low CNS transduction in our study, such as gender, since it has been reported that IV AAV9 infusion seems to have an androgen dependent effect, with vector preferentially transducing the liver in male mice, but favors the CNS in female mice [55,59]. Variables such as age at vector administration, dose, promoter, and AAV purification methods could also contribute to the differences observed in CNS transduction profile in different studies [37,38,54,60–62].

Intravenous administration of Laronidase ERT at normal doses in MPS I mice does not prevent pathology in the brain due to inability of enzyme to cross the blood brain barrier [16,63]. However, Ou et al. [64] have shown that when multiple high doses of enzyme were administered intravenously in MPS I mice there was improvement in neurobehavioral performance and reduction in GAG accumulation in the brain. These results indicate that maintenance of enzyme at high levels in the circulation allows at least some enzyme to penetrate the blood brain barrier by a mechanism that is as yet unknown. Several other studies of high dose enzyme replacement have been conducted in other lysosomal disease models with similar results [65–67]. In addition, Laoharawee et al. [68] and Ou et al. [34] in 2 separate studies demonstrated that high levels of circulating iduronate sulfatase or IDUA after ZFN-mediated gene editing and liver-specific expression resulted in enzyme delivery and reduced GAG in the brain, thereby preventing the emergence of neurological deficit in MPS II and MPS I, respectively. Because the liver was the only source of enzyme, these studies show that a consistent, high level of secretion into the circulation can result in enzyme delivery to the brain as a remedy for these lysosomal diseases.

Our data suggest that the high levels of IDUA enzyme activity observed in the brain with both AAV serotypes come not from transduction of neural cells but from supraphysiological levels of circulating IDUA that subsequently crosses the BBB. While the high levels of IDUA enzyme activity in the brain were accompanied by a significant reduction of GAGs compared to untreated mice, GAG levels were not completely normalized. Another potential mechanism of delivery is suggested by the putative expression of IDUA in pericytes of the CNS vasculature. Since the brain is highly vascularized, this may promote a bystander effect in which a portion of lysosomal protein that is secreted by transduced cells is taken up by neighboring cells on the parenchymal side of the BBB [69,70], thereby leading to normalized levels of IDUA activity observed throughout the brain. Similarly, IDUA expressed by the vasculature of the choroid plexus may gain access to the CSF.

This is the first study reporting therapeutic efficiency after intravenous delivery of AAV9 and AAVrh10 vectors encoding IDUA in adult MPS I mice. We show widespread and high-level expression of IDUA in multiple tissues including the brain after a single injection of AAV vector, with reduced GAG in tissues and urine. Our findings indicate that in the mouse MPS I model, most of the enzyme delivered to the brain most likely comes from the plasma after high level secretion from the liver. AAV 9 and AAV rh10 were equally effective in restoring enzyme activity and reducing GAG storage systemically. These results demonstrate that intravenous administration of AAV9 or AAVrh10 encoding IDUA is a potentially effective treatment for MPS I patients using a minimally invasive approach.

Acknowledgements

This study was funded by NIH grant P01 HD032652 to the University of Minnesota and NIH grant R41 DK094538 to REGENXBIO Corporation.

References

[1] E.F. Neufeld, J. Muenzer, The mucopolysaccharidoses, in: A.L. Beaudet, C.R. Scriver, W.S. Sly, D. Valle (Eds.), The Metabolic and Molecular Bases of Inherited Disease, McGraw Hill, New York, 2001, pp. 3421–3452.
[2] J. Muenzer, Overview of the mucopolysaccharidoses, Rheumatol 50 (2011) v4–v12.
[3] J.E. Wraith, S. Jones, Mucopolysaccharidosis type I, Pediatr. Endocrinol. Rev. 12 (2014) 102–106.
[4] W. Krivit, J.H. Sung, E.G. Shapiro, et al., Microglia: the effector cell for reconstitution of the central nervous system following bone marrow transplantation for lysosomal and peroxisomal storage diseases, Cell Transplant. 4 (1995) 385–392.
[5] W. Krivit, Allogeneic stem cell transplantation for the treatment of lysosomal and peroxisomal metabolic diseases, Springer Seminars Immunopathol. 26 (2004) 119–132.
[6] P.J. Orchard, B.R. Blazar, J. Wagner, et al., Hematopoietic cell therapy for metabolic disease, J Pediatrics 151 (2007) 340–346.
[7] D.C. Hess, T. Abe, W.D. Hill, et al., Hematopoietic origin of microglial and perivascular cells in brain, Exp. Neurol. 186 (2004) 134–144.
[8] V.K. Prasad, J. Kurtzberg, Transplant outcomes in mucopolysaccharidoses, Semin. Hematol. 47 (2010) 59–69.
[9] C. Peters, M. Balthazor, E.G. Shapiro, et al., Outcome of unrelated donor bone marrow transplantation in 40 children with Hurler syndrome, Blood 87 (1996) 4894–4902.
[10] C.B. Whitley, K.G. Belani, P.N. Chang, et al., Long-term outcome of Hurler syndrome following bone marrow transplantation, Am J Med Genet 46 (1993) 209–2018.
[11] G. Souillet, N. Guffon, I. Maire, et al., Outcome of 27 patients with Hurler's syndrome transplanted from either related or unrelated haematopoietic stem cell sources, Bone Marrow Transplant. 31 (2003) 1105–1117.
[12] E. Kakkis, M. McEntee, C. Vogler, et al., Intrathecal enzyme replacement therapy reduces lysosomal storage in the brain and meninges of the canine model of MPS I, Mol. Genet. Metab. 83 (2004) 163–174.
[13] M. Rohrbach, J.T. Clarke, Treatment of lysosomal storage disorders: progress with enzyme replacement therapy, Drugs 67 (2007) 2697–2716.
[14] M.V. Munoz-Rojas, T. Vieira, R. Costa, et al., Intrathecal enzyme replacement therapy in a patient with mucopolysaccharidosis type I and symptomatic spinal cord compression, Am. J. Med. Genet. A 146A (2008) 2538–2544.
[15] P. Dickson, M. McEntee, C. Vogler, et al., Intrathecal enzyme replacement therapy: successful treatment of brain disease via the cerebrospinal fluid, Mol. Genet. Metab. 91 (2007) 61–68.
[16] D.J. Begley, C.C. Pontikis, M. Scarpa, Lysosomal storage diseases and the blood-brain barrier, Curr. Pharm. Des. 14 (2008) 1566–1580.
[17] I. Visigalli, S. Delai, L.S. Politi, et al., Gene therapy augments the efficacy of hematopoietic cell transplantation and fully corrects mucopolysaccharidosis type I phenotype in the mouse model, Blood 116 (2010) 5130–5139.
[18] D. Wang, W. Zhang, T.A. Kalfa, et al., Reprogramming erythroid cells for lysosomal enzyme production leads to visceral and CNS cross-correction in mice with Hurler syndrome, Proc. Natl. Acad. Sci. U. S. A. 106 (2009) 19958–19963.
[19] M. Dai, J. Han, S.S. El-Amouri, et al., Platelets are efficient and protective depots for storage, distribution, and delivery of lysosomal enzyme in mice with Hurler syndrome, Proc. Natl. Acad. Sci. U. S. A. 111 (2014) 2680–2685.
[20] I. Visigalli, S. Delai, F. Ferro, et al., Preclinical testing of the safety and tolerability of lentiviral vector-mediated above-normal alpha-L-Iduronidase expression in murine and human hematopoietic cells using toxicology and biodistribution good laboratory practice studies, Hum. Gene Ther. 27 (10) (2016 Oct) 813–829.
[21] D.A. Wolf, S. Banerjee, P.B. Hackett, et al., Gene therapy for neurologic manifestations of mucopolysaccharidoses, Expert Opin Drug Deliv 12 (2015) 283–296.
[22] S.D. Hartung, J.L. Frandsen, D. Pan, et al., Correction of metabolic, craniofacial, and neurologic abnormalities in MPS I mice treated at birth with adeno-associated virus vector transducing the human alpha-L-iduronidase gene, Mol Therap. 9 (2004) 866–875.
[23] N. Desmaris, L. Verot, J.P. Puech, et al., Prevention of neuropathology in the mouse model of Hurler syndrome, Ann. Neurol. 56 (2004) 68–76.
[24] S. Chung, X. Ma, Y. Liu, et al., Effect of neonatal administration of a retroviral vector expressing alpha-L-iduronidase upon lysosomal storage in brain and other organs in mucopolysaccharidosis I mice, Mol. Genet. Metab. 90 (2007) 181–192.
[25] A.M. Traas, P. Wang, X. Ma, et al., Correction of clinical manifestations of canine mucopolysaccharidosis I with neonatal retroviral vector gene therapy, Mol. Ther. 15 (2007) 1423–1431.
[26] D.A. Wolf, A.W. Lenander, Z. Nan, et al., Direct gene transfer to the CNS prevents emergence of neurologic disease in a murine model of muco- polysaccharidosis type I, Neurobiol. Dis. 43 (2011) 123–133.
[27] H. Kobayashi, D. Carbonaro, K. Pepper, et al., Neonatal gene therapy of MPS I mice by intravenous injection of a lentiviral vector, Mol. Ther. 11 (2005) 776–789.
[28] C.G. Janson, L.G. Romanova, P. Leone, et al., Comparison of endovascular and intraventricular gene therapy with adeno-associated virus-α-L-iduronidase for Hurler disease, Neurosurgery 74 (2014) 99–111.
[29] C. Hinderer, P. Bell, B.L. Gurda, et al., Intrathecal gene therapy corrects CNS pathology in a feline model of mucopolysaccharidosis I, Mol Ther 22 (2014) 2018–2027.
[30] C. Hinderer, P. Bell, J.P. Louboutin, et al., Neonatal systemic AAV induces tolerance to CNS gene therapy in MPS I dogs and nonhuman primates, Mol. Ther. 23 (2015) 1298–1307.
[31] N.M. Ellinwood, J. Ausseil, N. Desmaris, et al., Safe, efficient, and reproducible gene therapy of the brain in the dog models of Sanfilippo and Hurler syndromes, Mol. Ther. 19 (2011) 251–259.
[32] C. Hinderer, P. Bell, B.L. Gurda, et al., Liver-directed gene therapy corrects cardiovascular lesions in feline mucopolysaccharidosis type I, Proc. Natl. Acad. Sci. U. S. A. 111 (2014) 14894–14899.
[33] L.R. Belur, A. Temme, K.M. Podetz-Pedersen, et al., Intranasal adeno-associated virus mediated gene delivery and expression of human Iduronidase in the central nervous system: a noninvasive and effective approach for prevention of neurologic disease in mucopolysaccharidosis type I, Hum. Gene Ther. 28 (7) (2017 Jul) 576–587.
[34] L. Ou, R.C. DeKelver, M. Rohde, et al., ZFN-mediated in vivo genome editing corrects murine hurler syndrome, Mol. Ther. 27 (1) (2019 Jan 2) 178–187.
[35] J. Hordeaux, C. Hinderer, T. Goode, et al., Toxicology study of intra-cisterna magna adeno-associated virus 9 expressing human alpha-L-Iduronidase in rhesus macaques, Mol Ther Methods Clin Dev. 10 (2018 Jul 14) 79–88.
[36] J. Hordeaux, C. Hinderer, E.L. Buza, et al., Safe and sustained expression of human Iduronidase after intrathecal Administration of Adeno-Associated Virus Serotype 9 in infant rhesus monkeys, Hum. Gene Ther. 10 (2019 Jun).
[37] K.D. Foust, E. Nurre, C.L. Montgomery, et al., Intravascular AAV9 preferentially targets neonatal neurons and adult astrocytes, Nat. Biotechnol. 27 (1) (2009 Jan) 59–65.
[38] S. Duque, B. Joussemet, C. Riviere, et al., Intravenous administration of self-complementary AAV9 enables transgene delivery to adult motor neurons, MolTher. 17 (7) (2009 Jul) 1187–1196.
[39] B. Yang, S. Li, H. Wang, Y. Guo, et al., Global CNS transduction of adult mice by intravenously delivered rAAVrh.8 and rAAVrh.10 and nonhuman primates by rAAVrh.10, Mol. Ther. 22 (2014) 1299–1309.
[40] J.B. Rosenberg, D. Sondhi, D.G. Rubin, et al., Comparative efficacy and safety of multiple routes of direct CNS administration of adeno-associated virus gene transfer vector serotype rh.10 expressing the human arylsulfatase A cDNA to nonhuman primates, Hum. Gene Ther. Dev. 25 (2014) 164–177.
[41] S.J. Gray, V. Matagne, L. Bachaboina, et al., Preclinical differences of intravascular AAV9 delivery to neurons and glia: a comparative study of adult mice and nonhuman primates, Mol. Ther. 19 (2011) 1058–1069.
[42] H. Zhang, B. Yang, X. Mu, et al., Several rAAV vectors efficiently cross the blood-brain barrier and transduce neurons and astrocytes in the neonatal mouse central nervous system, Mol. Ther. 19 (2011) 1440–1448.
[43] J.R. Mendell, S. Al-Zaidy, R. Shell, et al., Single-dose gene-replacement therapy for spinal muscular atrophy, N. Engl. J. Med. 377 (18) (2017 Nov 2) 1713–1722.
[44] Charles H. Vite, Marco A. Passini, Mark E. Haskins, et al., Adeno-associated virus vector-mediated transduction in the cat brain, Gene Ther. 10 (2003) 1874–1881.
[45] Joana Duarte-Neves, Nélio Gonçalves, Janete Cunha-Santos, et al., Neuropeptide Y mitigates neuropathology and motor deficits in mouse models of Machado–Joseph disease, Hum. Mol. Genet. 24 (19) (2015) 5451–5463.
[46] J.B. Rosenberg, M.G. Kaplitt, B.P. De, et al., AAVrh.10-mediated APOE2 central nervous system gene therapy for APOE4-associated Alzheimer's disease, Hum Gene Ther Clin Dev. 29 (1) (2018) 24–47.
[47] J. Saraiva, R.J. Nobre, Pereira de Almeida L. gene therapy for the CNS using AAVs: the impact of systemic delivery by AAV9, J. Control. Release 241 (2016 Nov 10) 94–109.
[48] H. Fu, K. Zaraspe, N. Murakami, et al., Targeting root cause by systemic scAAV9-hIDS gene delivery: functional correction and reversal of severe MPS II in mice, Mol Ther Methods Clin Dev. 10 (2018 Sep 4) 327–340.
[49] S. Motas, V. Haurigot, M. Garcia, et al., CNS-directed gene therapy for the treatment of neurologic and somatic mucopolysaccharidosis type II (Hunter syndrome), JCI Insight 1 (9) (2016; Jun 16).
[50] V. Haurigot, S. Marcó, A. Ribera, et al., Whole body correction of mucopolysaccharidosis IIIA by intracerebrospinal fluid gene therapy, J. Clin. Invest. 1 (2013 Jul).
[51] K. Ohmi, D.S. Greenberg, K.S. Rajavel, et al., Activated microglia in cortex of mouse models of mucopolysaccharidoses I and IIIB, Proc. Natl. Acad. Sci. U. S. A. 100 (4) (2003) 1902–1907.
[52] H. Fu, A.S. Meadows, T. Ware, et al., Near-complete correction of profound Metabolomic impairments corresponding to functional benefit in MPS IIIB mice after IV rAAV9-hNAGLU gene delivery, MolTher. 25 (3) (2017 Mar 1) 792–802.
[53] B.L. Gurda, De Guilhem, De Lataillade a, Bell P, et al. evaluation of AAV-mediated gene therapy for central nervous system disease in canine Mucopolysaccharidosis VII, MolTher. 24 (2) (2016 Feb) 206–216.
[54] C.M. Weismann, J. Ferreira, A.M. Keeler, et al., Systemic AAV9 gene transfer in adult GM1 gangliosidosis mice reduces lysosomal storage in CNS and extends lifespan, Hum. Mol. Genet. 24 (15) (2015 Aug 1) 4353–4364.
[55] J.S. Walia, N. Altaleb, A. Bello, et al., Long-term correction of Sandhoff disease following intravenous delivery of rAAV9 to mouse neonates, Mol. Ther. 23 (2015) 414–422.
[56] C. Spampanato, E. De Leonibus, P. Dama, et al., Efficacy of a combined intracerebral and systemic gene delivery approach for the treatment of a severe lysosomal storage disorder, Mol. Ther. 19 (5) (2011) 860–869.
[57] N. Miyake, K. Miyake, N. Asakawa, et al., Long-term correction of biochemical and neurological abnormalities in MLD mice model by neonatal systemic injection of an

AAV serotype 9 vector, Gene Ther. 21 (2014) 427–433.
[58] C.A. Maguire, M.H. Crommentuijn, D. Mu, et al., Mouse gender influences brain transduction by intravascularly administered AAV9, Mol. Ther. 21 (8) (2013) 1470–1471.
[59] A.K. Bevan, S. Duque, K.D. Foust, et al., Systemic gene delivery in large species for targeting spinal cord, brain, and peripheral tissues for pediatric disorders, Mol Ther. 19 (11) (2011) 1971–1980.
[60] R.L. Klein, R.D. Dayton, J.B. Tatom, et al., AAV8, 9, Rh10, Rh43 vector gene transfer in the rat brain: effects of serotype, promoter and purification method, Mol. Ther. 16 (1) (2008) 89–96.
[61] E. Ayuso, et al., High AAV vector purity results in serotype- and tissue-independent enhancement of transduction efficiency, Gene Ther. 17 (4) (2010) 503–510.
[62] G.M. Enns, S.L. Huhn, Central nervous system therapy for lysosomal storage disorders, Neurosurg. Focus. 24 (2008) 3–4.
[63] L. Ou, T. Herzog, B.L. Koniar, et al., High-dose enzyme replacement therapy in murine hurler syndrome, Mol. Genet. Metab. 111 (2) (2014 Feb) 116–122.
[64] C. Vogler, B. Levy, J.H. Grubb, et al., Over- coming the blood–brain barrier with high-dose enzyme replacement therapy in murine mucopolysaccharidosis VII, Proc. Natl. Acad. Sci. U. S. A. 102 (2005) 14777–14782.
[65] J. Blanz, S. Stroobants, R. Lüllmann-Rauch, et al., Reversal of peripheral and central neural storage and ataxia after recombinant enzyme replacement therapy in alpha-mannosidosis mice, Hum. Mol. Genet. 17 (2008) 3437–3445.
[66] U. Matzner, R. Lüllmann-Rauch, S. Stroobants, et al., Enzyme replacement improves ataxic gait and central nervous system histopathology in a mouse model of metachromatic leukodystrophy, Mol. Ther. 17 (2009) 600–606.
[67] K. Laoharawee, R.C. DeKelver, K.M. Podetz-Pedersen, et al., Dose-dependent prevention of metabolic and neurologic disease in murine MPS II by ZFN-mediated in vivo genome editing, Mol. Ther. 26 (4) (2018 Apr 4) 1127–1136.
[68] J.C. Fratantoni, C.W. Hall, E.F. Neufeld, Hurler and Hunter syndromes: mutual correction of the defect in cultured fibroblasts, Science 162 (1968) 570–572.
[69] S. Kornfeld, Trafficking of lysosomal enzymes, FASEB J. 1 (1987) 462–468.
[70] D.J. Schuster, J.A. Dyskstra, M.S. Riedl, et al., Biodistribution of adeno-associated virus serotype 9 (AAV9) after intrathecal and intravenous delivery in mouse, Front. Neuroanat. 8 (2014) 42.